



Natural organic matter fouling using a cellulose acetate copolymer ultrafiltration membrane

Cesar García^a, Eduardo Rogel-Hernández^a, Shui Wai Lin^b, Heriberto Espinoza-Gómez^{a*}

^aFacultad de Ciencias Químicas e Ingeniería, Universidad Autónoma de Baja California-Tijuana, Calzada Tecnológico 14418, CP 22340, Del. Mesa de Otay, Tijuana, BC México

Tel: 52 664 979 7500, ext. 54300; email: jhespinoza@uabc.mx

^bCentro de Graduados del Instituto Tecnológico de Tijuana, Apdo. Postal 1166, Tijuana, BC México

Received 4 June 2007; Accepted 25 August 2008

ABSTRACT

The low molecular weight cut-off ultrafiltration process has become acceptable for drinking water treatment; however, irreversible fouling curtails the economic viability of such process. The objective of this study was to evaluate the effectiveness of an ultrafiltration membrane on natural organic matter rejection and the components of natural water that contribute to fouling. Membranes with different molecular weight cut-off were employed. Experimental solutions consist of natural organic matter isolated from natural water or humic substances. The experimental solutions were prefiltered and diluted to prevent cake formation on membrane and change the fouling mode to pore blockage. The aggregation rejection caused irreversible fouling of the 100 kDa membrane, presumably a result of pore size reduction due to internal deposition aggregates. The solution showed differences in rejection, flux decline and membrane resistance.

Keywords: Natural organic matter, Cellulose acetate; Copolymers; Ultrafiltration membrane; NOM; UF fouling

1. Introduction

Organic fouling is usually discussed in terms of adsorption of various natural organic materials on and in the membrane. Many studies suggested that natural organic matter (NOM) was the most important foulant [1]. Dissolved NOM (DOM) is usually considered to be all carbon-containing matters that pass through a submicron-sized filter (typically a 0.45- μ m pore size membrane). Recent studies suggested that NOM that causes the majority of adsorptive fouling during ultrafiltration was actually a small percentage of all the dissolved organic carbon in several river water supplies [2,3].

Humic substances (HS) are a particular group of contaminants that are present in water supplies and are

important in the water industry. The HS are a combination of humin, humic acid (HA) and fulvic acid (FA).

The application of UF technique to remove HA and other organic matter has been investigated by a number of researchers [4–6]. Direct adsorption measurements of HS onto hydrophobic UF membranes were carried out by Jucker and Clark [7]. Moreover, upon adsorption of HS, the membrane becomes more hydrophilic and apparent pore charge becomes less negative [8]. However, adsorption kinetics is faster for FA than for HA, mainly because the diffusivity is greater for small molecules than for large ones [9]. Kinetic studies by Maartens et al. [5] showed that adsorption of HA was slower than that of NOM. Also, adsorption is greater at pH 7 because the charge on HS is less negative, there is less repulsion among adsorbing molecules and charge repulsion between the negatively charged membrane and the HS molecule is lowered. This could also indicate that

*Corresponding author.

adsorption might only be an initial phenomenon, after which deposition would be due to precipitation or aggregation [10–13].

Küchler and Miekeley [4] studied UF of humic compounds through a 1 k Dalton membrane. It was observed that humic acid (HA) retention (80–90%) was greater than that of fulvic acid (FA) (60–70%). An opposite view was provided by Carroll et al. [14]; they concluded that the greatest degree of fouling was by smaller MW molecules. Crozes et al. [15] also showed that the momentary accumulation of particulate or organic matter on the membrane surface does not necessarily lead to irreversible fouling of the membrane. Irreversible fouling during filtration of natural waters seemed to be the result of a much slower process.

The main objective of this research is to investigate the fouling mode of a UF cellulose acetate copolymer membrane in the filtration of HA and DOC present in the Alamar River in Tijuana, México. Membrane pore size and HA concentration were varied during the experimental stages to investigate their effect on HA UF.

2. Materials and methods

2.1. Materials

The chemicals used were of analytical grade and supplied by Fluka (Sigma-Aldrich). Milli-Q water of a quality greater than 18 MW/cm was used for all solution preparations and experiments. The membranes used in this study were flat-disc UF membranes. They are asymmetric regenerated cellulose membranes (RC) with polyvinylpyrrolidone (90 kDa), supported in propylene, and are considered hydrophilic in nature; these membranes were provided by a local dealer. Membranes of MWCOs between 50–300 kDa were chosen. The characteristics are summarized in Table 1.

2.2. Filtration procedure

All the experiments were carried out in a dead-end stirred batch cell (volume of 110 mL and membrane area of $1.5 \times 10^{-3} \text{ m}^2$) pressurized with high purity nitrogen gas and stirred at 270 rpm. A feed reservoir of 2 L was connected to the stirred cell to provide extent filtration volumes.

Five hundred mL of feed solution were prepared and 50 mL were sampled. The rest of the feed solution was introduced into the reservoir. Pressure was adjusted to 100 kPa and the filtration cell was filled. The permeate was sampled and then recycled into the reservoir together with the retentate. Filtration was repeated two more times. This recycling experiment enabled the separation of concentration polarization effects from fouling effects. The

110 mL of retentate were then also sampled. In order to determine the extent of irreversible fouling; 1000 mL of Milli-Q water was filtered through the membrane at the same operating pressure after each experiment.

2.3. Natural organic matter solutions

NOM was isolated from the Alamar River in Tijuana City, Mexico. First, raw water was prefiltered through glass fiber filters to remove particulate matter, followed by pretreatment with a cartridge to reduce turbidity and then using a $0.45 \mu\text{m}$ PES membrane under vacuum pressure to concentrate all surface water constituents. The concentrate was further freeze-dried. The NOM powder obtained includes all inorganic salts and hydrophilic organics which are part of the surface water. Adsorption on XAD resins was chosen to obtain three fractions of this NOM of different hydrophobicity, a humic acid fraction (NOM-HA) a fulvic acid fraction (NOM-FA) and a hydrophilic fraction (NOM-Hyd). For NOM-HA, the pH was adjusted to 1.0 using hydrochloric acid, and the conductivity was adjusted to 5.3 mS/cm using sodium chloride. This source water had a dissolved organic carbon content of about 4.5 mg L^{-1} , and was denoted as DOC1.

Synthetic feed solutions were prepared using DOC1 and HA powder supplied from Sigma Aldrich and Milli-Q water as solvent. These solutions reflect various feedwater conditions [16–18] organic composition: (a) 280 mg L^{-1} NOM (DOC1 0%); (b) 70 mg L^{-1} NOM (DOC1 70%); and (c) 140 mg L^{-1} NOM (DOC1 30%)

2.4. Quantitative determination of NOM

The presence of unsaturated compounds usually imparts a distinct color to the contaminated water, and ultraviolet/visible light spectroscopy can therefore be used to estimate the absorbing compounds concentration. This strong light absorption at short wavelength can be attributed to the benzoide bands of carboxyphenols present in organics.

Spectrometric determinations were carried out using a DR 5000 UV/Vis spectrophotometer. Each sample was scanned from 190 to 500 nm, the wavelength of 254 nm being used to calculate rejection. All samples were measured against a Milli-Q water reference without pH adjustment, following the suggested standard method for surface water analysis [19].

2.5. Calculations

Membrane flux was calculated by Eq. (1).

$$J = \frac{1}{A} \frac{dV}{dt} \quad (1)$$

Table 1
Membrane characteristics

MWCO (kDa)	50	100	200	300
Pore diameter (nm)	7.5	15.1	21.2	28.3
operating pressure (kPa)	300	175	100	75
Average pure water flux (Lm ⁻² h ⁻¹)	75±5	210±4	467±9	680±2
Clean water permeability (Lm ⁻² h ⁻¹ bar ⁻¹)	21.9	290.5	610.9	1905.3
Clean membrane resistance (m ⁻¹)	1.66×10 ¹⁰	0.9×10 ¹⁰	0.05×10 ¹⁰	0.002×10 ¹⁰

where A is the membrane area and V the permeate volume at time t . The flux behavior is given as the ratio of the flux after a volume V of permeate collected (J) to the initial flux at the beginning of the experiment (J_0).

The mass permeation flux during membrane filtration can be expressed in terms of a resistance-in-series model as:

$$J_W = \frac{\Delta P}{R_M + R_{NOM}} = \frac{\Delta P}{R_T} \quad (2)$$

where J_W is the permeate flux, ΔP is the applied pressure, and R_T is the overall permeation resistance. In general, R_T comprises the membrane resistance, R_M , osmotic and concentration polarization effects, and effects of fouling. Because of the difficulty in separating fouling from osmotic and concentration polarization effects for NOM filtration, these phenomena are lumped together as R_{NOM} . However, we distinguish between the reversible ($R_{NOM,rev}$) and irreversible ($R_{NOM,irrev}$) components of R_{NOM} .

The measurement resistance was obtained from pure water flux measurements using Eq. (2) with $R_T=R_M$. Observed NOM rejection was calculated based on aggregate permeate and average feed concentrations (C_p and C_f , respectively) measured at 4.3, 20, and 30 kg m⁻² permeate throughput as follows:

$$\%R = 100 \left(1 - \frac{C_p}{C_f} \right) \quad (3)$$

For dead-end filtration under constant applied pressure, rate laws corresponding to pore blockage, pore constriction, and cake formation can be written by assuming that the either number of pores, the diameter of pores, or the mass cake layer formed at the membrane surface change in proportion to the convective transport of mass to the membrane surface. In conjunction with the standard filtration equation [Eq. (1)], various fouling models are obtained for each fouling mode, which can all be formulated as a single equations as proposed by Hermans and Bredee [20]:

$$\frac{d^2t}{dW^2} = k \left(\frac{dt}{dW} \right)^n \quad (4a)$$

$$\ln \left(\frac{d^2t}{dW^2} \right) - \ln k + n \ln \left(\frac{dt}{dW} \right) \quad (4b)$$

where t is time, W is the mass filtered, k is a fouling coefficient with units that depend on the value of n , and n is a dimensionless filtration constant that reflects the mode of fouling: (1) cake formation corresponds to $n = 0$; (2) complete pore blocking corresponds to $n = 2$; (3) standard pore blocking corresponds to $n = 1.5$ [21]. In Eq. (4), dt/dW is the differential times needed to collect a unit differential mass of permeate, $1/J_w A$. The d^2t/dW^2 term on the left-hand side was calculated from $-(dJ_w/dt)/(A^2)^3$. Eq. (4b) is similar to the linear equation, where n is the line slope.

Ho and Zydney [22] developed a model for dead-end filtration of proteins that combines pore blockage and cake filtration modes of fouling. In this model, total flow through the membrane at any time during filtration, Q , is the sum of flow through open pores and through partially blocked pores on which a cake has formed. Assuming a uniform resistance of the fouling layer over the membrane surface, and in the absence of significant cross-flow, the combined pore blockage-cake filtration model is written

$$Q = Q_0 \left\{ \exp \left(- \frac{\alpha_b \Delta P C_F t}{R_M} \right) + \frac{R_M}{R_M + R_C} \left[1 - \exp \left(- \frac{\alpha_b \Delta P C_F t}{R_M} \right) \right] \right\} \quad (5)$$

where α_b is the pore blockage parameter; note that C_F is in weight fraction units. The resistance from cake formation, R_C , which increases as a function of time in proportion to the rate that NOM mass accumulates on the membrane surface, is obtained from

$$\frac{R_M + R_C}{R_M + R_{C,0}} = \sqrt{1 + \frac{2\alpha_c \Delta P C_F}{(R_M + R_{C,0})^2} t} \quad (6)$$

where α_c is the cake formation parameter and $R_{C,0}$ is the initial resistance of the deposit (i. e., a leakage flow). Ho

and Zydney [22] discuss an approach to explicitly account for the variation in the cake layer resistance over the surface of the membrane but showed that this approach yields results similar to Eqs. (4) and (5). It should be noted that they treated C_f as constant. Increases in C_f during a run were on the order of zero to a few percent for the larger MWCO membranes and up to about 20% for the smaller pore size membranes. When t is small ($t \ll R_M \alpha_b \Delta PC_b$) is equivalent to the classical pore blockage model. At long times ($t \gg R_M \alpha_b \Delta PC_b$), the volumetric flux is governed by the classic cake filtration model [23].

Best-fit values of the pore blockage parameter, α_b , specific cake resistance parameter, α_c , and resistance of the initial fouling layer, $R_{c,0}$, were obtained by minimizing the sum of squared residuals between the model and the data. In addition, because the model was sensitive to values of Q_0 , this parameter was also adjusted to optimize the model fit. Parameter sets determined by minimizing the sum of squares between model and experimental fluxes appear to be unique, likely because each parameter has a different effect on the flux decline curve. The combined pore blockage/cake filtration model was used to evaluate the derivatives in Eq. (4) making it possible to accurately track the value of the filtration constant during a run and to identify how the dominant mode of fouling evolves during filtration.

3. Results and discussion

Raw water was used directly in one filtration test for comparison. Prefiltered raw water through a glass-fiber filter to remove particulates was used for a similar filtration test. The flux decline in the two tests identifies the relative contribution of fouling by dissolved and particulate matter. An example of the results from these experiments is shown in Fig. 1. Raw and prefiltered solutions both fouled 200 kDa UF membranes rapidly, but the extent of fouling was slightly worse for the solution containing particulate matter. The flux decline during each experiment is calculated from initial and final flux values:

$$\Phi = 1 - \frac{J_F}{J_0} \quad (7)$$

where Φ is the flux decline and the subscripts 0 and F refer to initial and final values, respectively. After filtration of 100 L m⁻² of water, the water without particulate matter caused an 80% flux decline, and the water with particulate matter caused a 90% flux decline.

After prefiltration through the glass fiber filter, the source water concentration contained 4.5 mg L⁻¹ of DOC, it was monitored during the experiments shown in Fig. 2,

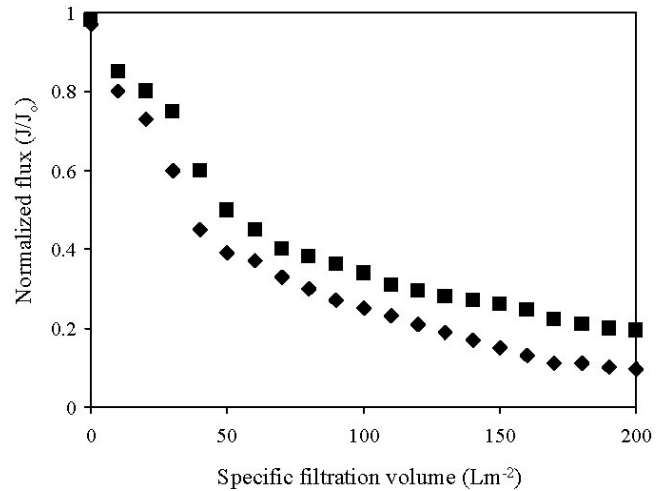


Fig. 1. Permeate flux of Alamar River through 200 kDa membranes with and without prefiltration. Prefiltered (■), Raw (◆).

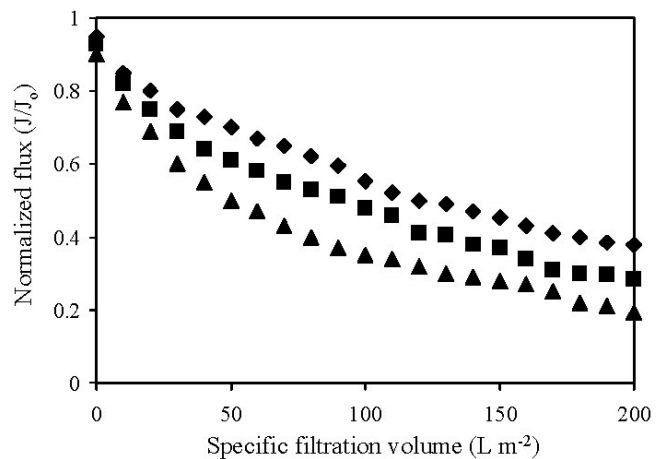


Fig. 2. Permeate flux of Alamar River water through 0.2 μm polypropylene membranes after fractionation through regenerated cellulose membranes with various pore sizes. 100 kDa (◆), 200 kDa (■), 300 kDa (▲).

and rejection was calculated using Eq. (3). Rejection of DOM by the RC membranes was low: 6% for membranes with 300 kDa, 15% for the membranes with 200 kDa, and 20% for membranes with 100 kDa MWCO. The permeate flux is shown in Fig. 2. Regenerated cellulose is unlikely to retain material by adsorption or mechanisms other than size exclusion [23]. Surface cake formation was minimized by removing particulate matter in the prefiltration step.

The membrane resistance rate change is tabulated as a function of permeate throughput, dR_T/dW , for the feed solutions (Table 2). For the 140 mg L⁻¹ NOM (30% DOC1), the rate of change in the resistance was essentially constant after an initial period (Fig. 3a). For loading greater than 10 kg m⁻², the dR_T/dW values reached a constant value of $0.17 \pm 0.02 \times 10^6$ m⁴ Pas kg⁻² (Table 2). The constant

Table 2

Average change in differential resistance per mass of permeates filtered at steady state

Membrane MWCO (kDa)	$\frac{dR_T}{dW}$ [=] $\times 10^6 \text{ m}^4 \text{ Pa s kg}^{-2}$		
	(280 mg L ⁻¹)	(70 mg L ⁻¹)	(140 mg L ⁻¹)
50	0.15 ± 0.02	0.07 ± 0.001	0.11 ± 0.05
100	0.18 ± 0.01	0.06 ± 0.002	0.10 ± 0.02
200	0.17 ± 0.02	0.05 ± 0.001	0.11 ± 0.03
300	0.18 ± 0.02	0.07 ± 0.005	—
Mean $\frac{dR_T}{d+W}$	0.17 ± 0.02	0.063 ± 0.003	0.11 ± 0.04

rate of change in the resistance implies the filtration constant (n) in Eq. (4) is equal to zero, consistent with fouling by cake formation, and the rate of fouling by cake formation ($t/t_{\max} > 0.50$) was independent of the membrane pore size. This is agreeing with the findings of Yuan et al. [24] and Taniguchi et al. [21].

The data in Table 2 reveal that dR_T/dW was not constant for membranes up to MWCO 200 kDa, while the rate of fouling by cake formation was reduced by a factor of 2, between NOM 70 mg L⁻¹ HA (70% DOC1) and NOM 140 mg L⁻¹ (30% DOC1) ($dR_T/dW = 0.063 \pm 0.003 \times 10^6 \text{ m}^4 \text{ s Pa kg}^{-2}$), ($dR_T/dW = 0.11 \pm 0.04 \times 10^6 \text{ m}^4 \text{ s Pa kg}^{-2}$).

Permeation resistance is shown as a function of reduce time, t/t_{\max} , for the sample of water in Fig. 3(a–c). Actual time t was normalized by the time required to process $\sim 30 \text{ kg m}^{-2}$ of NOM solution, t_{\max} , because the length of a filtration run decreased with increasing membrane MWCO, degree of pretreatment, and dilution of the feed. Resistance was plotted as a function of time rather than mass throughput to facilitate fitting the combined pore blockage–cake formation model [Eqs. (5) and (6)].

Water prefiltration reduced the rate of fouling of the 300 kDa membrane, and the fouling was not dominated by cake formation (Fig. 3c). These findings are consistent with the data presented by Yuan and Zydney [24].

The reversibility of NOM fouling (by backwashing) is shown in Fig. 4. The reversible resistance after filtration of the 280 mg L⁻¹ NOM (0% DOC1) was independent of membrane MWCO. This supports an interpretation of the reversible resistance as that contributed by the formation of a cake layer on the membrane surface and is consistent with the ability of aggregates to catalyze fouling by cake formation.

Fig. 5 shows the relation between $\left(\frac{d^2t}{dw^2}\right)$ vs $\left(\frac{dt}{dw}\right)$.

Considering that n is a dimensionless filtration constant that reflects the mode of fouling: (1) cake formation corresponds to $n = 0$; (2) complete pore blocking corresponds

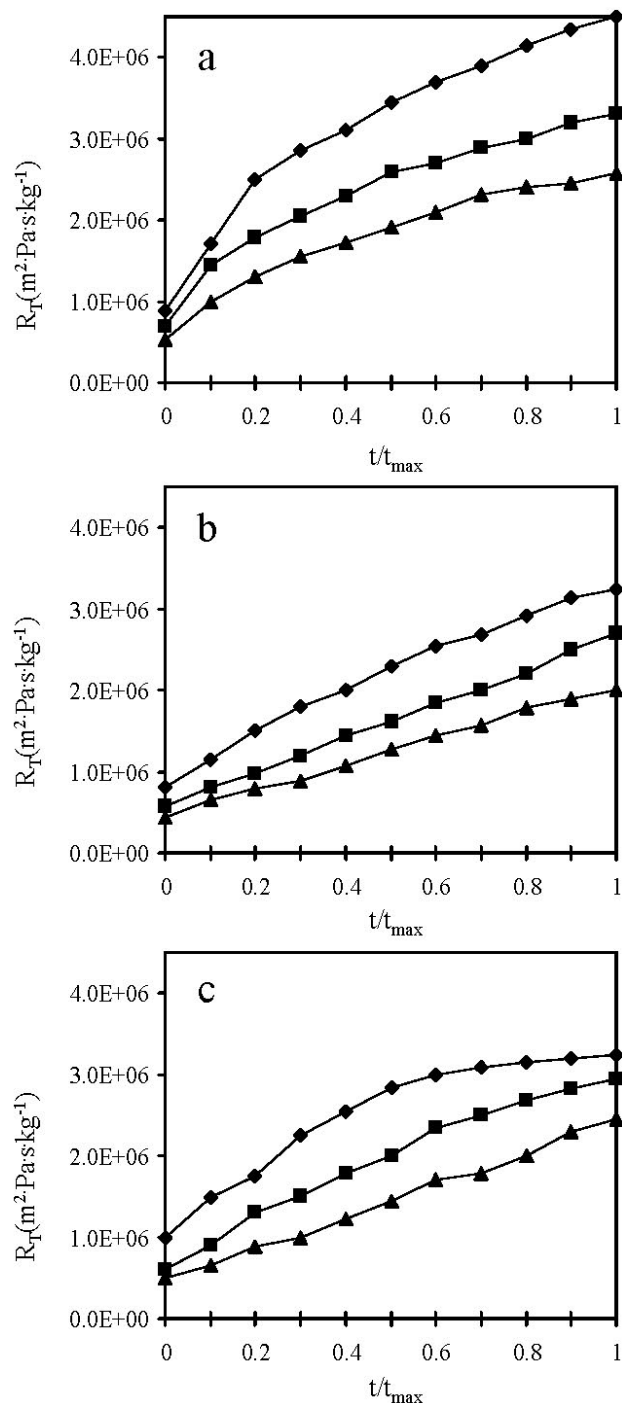


Fig. 3. Effect of membrane MWCO on the development of total resistance as a function of reduced time, t/t_{\max} ; t_{\max} is time to filter 30 kg m^{-2} NOM feed solution. Feed solutions: (a) 140 mg L⁻¹ NOM (30% DOC1); (b) 70 mg L⁻¹ NOM (70% DOC1); (c) 280 mg L⁻¹ NOM (0% DOC1). Membrane MWCOs: 300 kDa (▲); 200 kDa (■); 100 kDa (◆).

to $n=2$; (3) standard pore blocking corresponds to $n = 1.5$ [21], we can observe that the fouling mode did not correspond to cake formation.

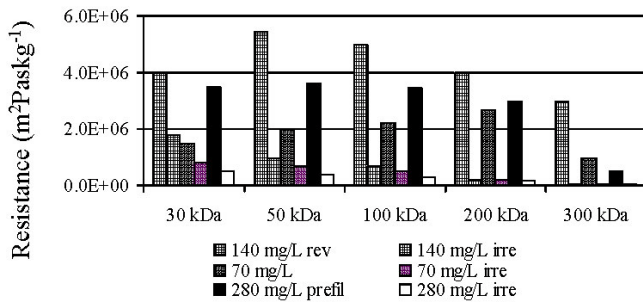


Fig. 4. Comparison of reversible (removed by backwashing) and irreversible resistances after filtration: 140 mg L⁻¹ NOM (30% DOC1): downward dash (reversible), upward dash (irreversible); 70 mg L⁻¹ NOM (70% DOC1): downward diagonal (reversible), upward diagonal (irreversible); and 280 mg L⁻¹ NOM (0% DOC1) (0.45 μm) RO isolate: solid bar (reversible), unfilled bar (irreversible).

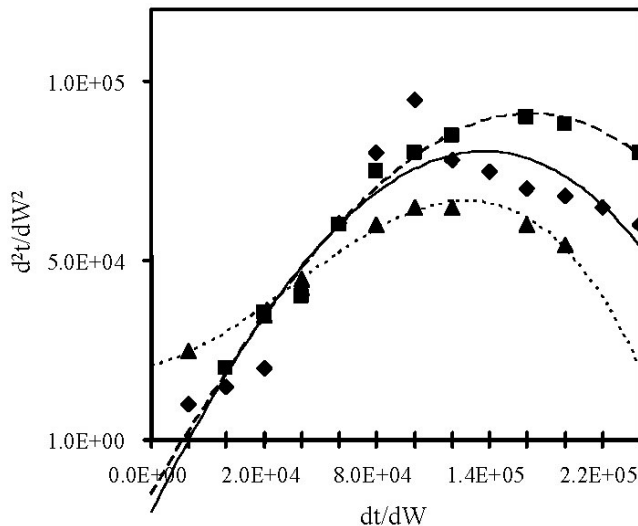


Fig. 5. Filtration data for 70 mg/L and 70% of HA. Lines are derivatives calculated from the combined formation model. Log slope of plot yields the filtration constant, n . Membrane MWCOs: 300 kDa (▲); 200 kDa (◆); 100 kDa (■).

4. Conclusions

In this study, the fouling of UF membranes due to different synthetic feed solutions was studied. After filtration of 100 L m⁻² of water across a 200 kDa UF membrane, the water without particulate matter caused an 80% flux decline, and the water with particulate matter caused a 90% flux decline. Rejection of DOM by the RC membranes was low for membranes with high MWCO. The dR_T/dW was not constant for the larger MWCO membranes; this suggested a different mode of fouling, instead of fouling by cake formation ($n \neq 0$) [21]. The reversible resistance after filtration of the 280 mg L⁻¹ NOM (0% DOC1) was independent of membrane MWCO. This

correlates with the mode of fouling, which did not shift fully to cake formation for the larger MWCO membranes. Similar trends were observed for the reversible component of resistance after filtration of the 70 mg L⁻¹ NOM (70% DOC1) removal of aggregates prevented cake formation and either significantly reduce (300 kDa membrane) reversible fouling. Irreversible fouling was observed with smaller MWCO membranes (MWCO up to 100 kDa), a finding consistent with that of Cho et al. [25] for filtration of prefiltered surface waters with a 10 kDa PES UF membrane. These NOM components contributed to pore blockage and were difficult to remove, perhaps due to steric hindrance. However, pore blockage was not a dominant fouling mode, and the irreversible resistance was a relatively small fraction of the total resistance. Irreversible fouling was reduced by both dilution and prefiltration of the feed. Apparently, prefiltration to remove aggregates also removed some of the more reactive species that contributed to irreversible fouling.

5. Symbols

A	—	Membrane area, m ²
C_b	—	Bulk concentration (concentration in the batch cell), mg L ⁻¹
C_f	—	Feed concentration, mg L ⁻¹
C_p	—	Permeate concentration, mg L ⁻¹
$C_{p,i}$	—	Permeate concentration of i , mg L ⁻¹
C_R	—	Concentration in the cell at the end of the experiment, mg L ⁻¹
dt/dW	—	Differential times needed to collect a unit differential mass of permeate
J	—	Flux, L m ⁻² h ⁻¹
J_F	—	Final flux, L m ⁻² h ⁻¹
J_0	—	Initial flux, L m ⁻² h ⁻¹
J_w	—	Permeate flux, kg m ⁻² s ⁻¹
K	—	Fouling coefficient
Mass	—	Deposit of solute in the membrane surface, mg
ΔP	—	Applied pressure, Pa
Q	—	Total flow through the membrane at any time during filtration, kg s ⁻¹
Q_0	—	Flow through the membrane at initial time, kg s ⁻¹
RC	—	Resistance for cake formation, Pa m ² s kg ⁻¹
$R_{c,0}$	—	Initial resistance of the deposit, Pa m ² s kg ⁻¹
R_M	—	Osmotic and concentration polarization and effects of fouling, Pa m ² s kg ⁻¹
R_{NOM}	—	NOM permeation resistance, Pa m ² s kg ⁻¹
$R_{NOM,rev}$	—	NOM permeation resistance (reversible), Pa m ² s kg ⁻¹
$R_{NOM,rev,i}$	—	NOM permeation resistance (irreversible), Pa m ² s kg ⁻¹

- R_T — Overall permeation resistance, Pa m²s kg⁻¹
 T — Time, s
 V — Permeate volume (mL)
 V_f — Volume of feed (mL)
 $V_{p,i}$ — Volume of permeate i (mL)
 V_r — Volume left in the cell at the end of the experiment, mL
 W — Mass filtered, kg

Greek

- α_b — Pore blockage parameter, m² kg⁻¹ solute
 α_c — Cake formation parameter, Pa m⁴ s kg⁻²
 Φ — Flux decline

Acknowledgement

This research was funded by the Universidad Autónoma de Baja California through grant 3820/10a.

References

- [1] K.J. Howe and M.M. Clark, *Environ. Sci. Technol.*, 36 (2002) 3571–3576.
- [2] E. Aoustin, A.I. Schäfer, A.G. Fane and T.D. Waite, *Sep. Purif. Technol.*, 22 (2001) 63–68.
- [3] K.J. Howe and M.M. Clark, *Coagulation pretreatment for membrane filtration*, AWWA and American Water Works Research Foundation, Denver, 2003.
- [4] I.L. Küchler and N. Miekeley, *Sci. Total Environ.*, 154 (1994) 23–28.
- [5] A. Maartens, P. Swart and E.P. Jacobs, *Desalination*, 115 (1998) 215–227.
- [6] K. Glucina, A. Alvarez and J.M. Laine, *Desalination*, 132 (2000) 73–82.
- [7] C. Jucker and M.M. Clark, *J. Membr. Sci.*, 97 (1994) 37–52.
- [8] E. Tipping and M. Ohnstad, *Chem. Geol.*, 44 (1982) 349–357.
- [9] P.K. Cornel, R.S. Summers and P.V. Roberts, *J. Coll. Interface Sci.*, 110 (1986) 149–164.
- [10] A.I. Schäfer, A.G. Fane and T.D. Waite, *Desalination*, 108 (1998) 109–122.
- [11] F.A. Bonner, J.L. Bersillon and C.R. O'Melia, *Proc. AWWA Annual Conference, Vancouver, 1992*, pp. 18–22.
- [12] A.J.V. van Boxtel, Z.E.H. Otten and H.J.L.J. van der Linden, *J. Membr. Sci.*, 58 (1991) 89–111.
- [13] J.M. Laine, J.P. Hagstrom and M.M. Clark, *J. AWWA*, 81 (1989) 61–67.
- [14] T. Carroll, S. King, S.R. Gray, B.A. Bolto and N.A. Booker, *Water Res.*, 35 (2000) 2861–2868.
- [15] G. Crozes, J. Jacangelo and C. Anselme, *J. Membr. Sci.*, 84 (1993) 61–77.
- [16] J.E. Kilduff, S. Mattaraj, J. Sensibaugh, J.P. Pieracci and G. Belfort, *Desalination*, 132 (2000) 133–142.
- [17] A. Braghetta, F.A. DiGiano and W.P. Ball, *J. Environ. Eng.*, 123 (1997) 628–641.
- [18] A. Braghetta, F.A. DiGiano and W.P. Ball, *J. Environ. Eng.* 124 (1998) 1087–1098.
- [19] A. Eaton, *J. AWWA*, 47 (1995) 86–90.
- [20] P.H. Hermans and H.L. Bredee, *J. Soc. Chem. Ind.*, 55 (1936) 1T–4T.
- [21] M. Taniguchi, J.E. Kilduff and G. Belfort, *Environ. Sci. Technol.*, 37 (2003) 1676–1683.
- [22] C.C. Ho and A.L. Zydney, *J. Coll. Interface Sci.*, 232 (2000) 389–399.
- [23] M. Cheryan, *Ultrafiltration and Microfiltration Handbook*, Technomic, Lancaster, PA, 1998.
- [24] W. Yuan and A.W. Sydney, *Environ. Sci. Technol.*, 34 (2000) 5043–5050.
- [25] J. Cho, G. Amy and J. Pellegrino, *J. Membr. Sci.*, 33 (1999) 2517–2526.